

# 2018

25th International Lightning Detection Conference &  
7th International Lightning Meteorology Conference  
March 12 - 15 | Ft. Lauderdale, Florida, USA

## Upward Lightning Triggering Study (UPLIGHTS): Project Summary and Initial Findings

Tom A. Warner, Alana Ballweber, Ryan Lueck, and  
John H. Helsdon, Jr.  
Department of Physics  
South Dakota School of Mines and Technology  
Rapid City, South Dakota, USA  
tom.warner@ztresearch.com

Carina Schumann and Marcelo M. F. Saba  
National Institute for Space Research  
INPE  
San Jose dos Campos, Brazil

Julia Tilles and Ron Thomas  
Department of Physics  
New Mexico Institute of Mining and Technology  
Socorro, New Mexico, USA

Richard E. Orville  
Department of Atmospheric Sciences  
Texas A&M University  
College Station, Texas, USA

**Abstract—** The Upward Lightning Triggering Study (UPLIGHTS) took place in Rapid City, South Dakota, USA from 2012 through 2014. 38 upward flashes were observed during the summer thunderstorm months (Apr – Sep) with a combination of high- and standard-speed video and digital still cameras, electric field meters, fast antenna systems, and for the 2014 season, a Lightning Mapping Array. All upward flashes were triggered by preceding lightning activity with the +CG flash the dominate triggering type. Intracloud and post +CG return stroke negative leaders passing near the towers were the primary triggering flash component, 2.4 times more frequent than the +CG return stroke triggering component. The one observed upward negative leader was triggered by a preceding -CG return stroke.

**Keywords—**upward lightning, triggering, initiation

### I. INTRODUCTION

Understanding of upward lightning has evolved significantly over the last ten years due to research efforts around the world. Some of the research locations include Japan, Austria, Germany, Switzerland, Canada, USA, Brazil, China and South Africa.

Notable findings include the following: 1) upward lightning can initiate without preceding nearby lightning activity or can be triggered by preceding flashes [Wang et al., 2008; Wang and Takagi, 2012]. 2) Self-initiated upward lightning (SIUL) tends to occur more often in winter months with lower cloud bases, colder temperatures and with stronger winds, whereas lightning-

triggered upward lightning (LTUL) tends to occur more often during summer months with active storms that contain higher cloud bases and warmer temperatures. [Wang and Takagi, 2012; Zhou et al., 2012]. 3) A large majority of upward lightning involves the development of an upward propagating positive leader which is classified as upward negative lightning in the literature since negative charge is effectively lowered to ground [Miki et al., 2010; Zhou et al., 2012; Warner et al., 2012a; Smorgonskiy et al., 2015; Saba et al., 2016]. 4) The dominate storm type for LTUL is a Mesoscale Convective System (MCS) with an associated stratiform precipitation area over the tall objects that experience upward lightning [Warner et al., 2012b; Saba et al., 2012; Jiang et al., 2014; Yuan et al., 2017]. 5) A majority of LTUL is triggered by preceding horizontally extensive positive cloud-to-ground flashes [Zhou et al., 2012, Warner et al., 2012a; Schumann et al., 2014a, 2014b, 2015; Saba et al., 2012, 2016]. 6) Horizontally extensive flashes that trigger transient luminous events (TLEs) in the upper atmosphere can also trigger upward lightning during the same flash [Lyons et al., 2011; Lyons et al., 2012; Warner et al., 2012c; Lyons et al., 2014; Rison et al., 2014]. 7) Horizontal propagating negative leaders and/or positive cloud-to-ground return strokes that pass near or over tall objects are the primary triggering flash components responsible for initiating upward positive leaders (UPLs) [Mazur and Ruhnke, 2011; Warner, 2012; 2012a; 2012b; Saba et al., 2012, 2016; Schumann et al., 2014a, 2014b, 2014c]. 8) The development of an UPL can lead to the initiation of an upward negative leader (UNL) from a nearby object [Lu et al., 2009]. 9) Lightning-triggered UPLs frequently transition to

horizontal propagation just below cloud base and then branch extensively [Warner et al., 2012c; Schumann et al., 2014a; Saba et al., 2016].

This paper reports on the observations and initial findings from the Upward Lightning Triggering Study (UPLIGHTS) that took place in Rapid City, South Dakota, USA from 2012 – 2014. This study sought to further define and characterize the nearby lightning triggering process that leads to upward leader initiation and development from tall objects. We first summarize the observations made during the campaign, and then present a visual model of the triggering processes based on findings from our analyses. Using this framework, we then discuss specific LTUL examples relating to components and processes incorporated in the model. Findings from the analysis of weather conditions and charge distributions favorable for upward lightning during UPLIGHTS will be provided via separate papers at this conference.

## II. PROJECT SUMMARY

### A. Overview

UPLIGHTS utilized multiple optical assets that included high- and standard-speed video cameras along with digital still image cameras to record visual observations of triggering flashes and upward leader initiation and development. Electric field sensing equipment, which included fast antenna systems and electric field meters, provided data on the ambient electric field before as well as its change during upward flashes. The addition of a Lightning Mapping Array (LMA) for the 2014 season allowed for the 3-dimensional visualization of lightning leader development and propagation relative to the towers. The National Weather Service KUDX WSR-88D, located 35 km east of the towers, recorded weather radar data including dual-polarity data beginning with the 2013 season. The National Weather Service Forecast Office in Rapid City, located 3 km east of the closest tower, recorded meteorological surface data and upper air soundings twice daily (see Figure 1).

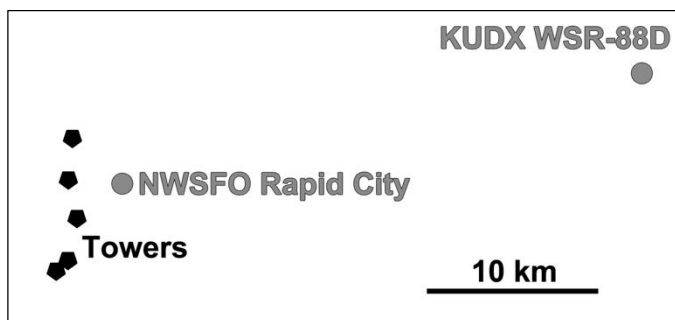


Figure 1. Layout of the 10 towers relative to the National Weather Service forecast office and weather radar.

### B. Instrumentation

Optical assets included high- and standard-speed video cameras along with digital still image cameras. Up to five high-speed cameras operating between 1,000 and 35,000 images per second (ips) were used to record lightning flash activity. Cameras were grouped into two mobile platforms, which were positioned at various locations from 600 m to 9 km from the

towers (see Figure 2). The two vehicles were spatially separated so that recordings could provide some level of 3-dimensionality when comparatively analyzed. Variable vehicle locations were chosen based on storm direction of movement, storm type and expected visibility. Each vehicle had at least two high-speed cameras with one having a wide field of view, and the other having a moderate field of view on selected towers. Each vehicle also had one camera that operated in the 1,000 – 2,000 ips range and another in the 10,000 – 35,000 ips range. The two vehicles also contained standard-speed video cameras recording in standard- and high-definition that provided 60 ips continuous video at extremely wide field of views and moderate field of views on selected towers. A single digital still camera located in each vehicle captured entire flashes employing continuous 10 second exposures at night. During the day, these cameras utilized an infrared trigger with the lens aperture set at f/8 and ISO at 100 resulting in images with “camera determined” exposure times based on ambient light conditions.

Three fixed optical sites located on opposing sides of Rapid City captured continuously recorded wide field of view standard-speed video at 60 ips as well as digital still images. Distances from these sites to each of the towers ranged from 2.5 km to 11 km.

The National Institute for Space Research (INPE), Brazil operated flat-plate, fast antenna systems with a sample rate of 5 million samples/second and a lower and upper frequency bandwidth of 306 Hz and 1.5 MHz respectively. Both a high- and low-gain fast antenna were placed together approximately 5 km west of the towers (West Sensors in Figure 2). At this location, the dual gain system provided increased dynamic range for sensing electric field changes primarily associated with triggering flashes. A low-gain fast antenna was placed between towers 1 and 2 (North Sensors in Figure 2). At this location, the sensor was within 1.6 km of the three towers that historically produced the most upward leaders (Towers 1, 4 and 6), optimizing the recording of both the triggering flash electric field change near the tower locations and the field change resulting from the development of the upward leaders.

Co-located with the fast antenna systems were rotating vane electric field meters (EFMs) that sampled the ambient electric field at 20 samples/second. An additional EFM was also located on one of the mobile vehicles. The field meters were factory-calibrated but were not calibrated to account for local field enhancement at each individual sensor site. Therefore, they were not absolutely calibrated so electric field magnitude could not be compared relatively between the three different site locations. Data obtained from the EFMs provided insight into the initial electric field polarity as well as direction and magnitude of change during upward flashes at varying distances and directions from the towers.

For the 2014 observation season, a nine-station LMA provided by New Mexico Tech was installed with the centroid approximately 50 km east-southeast of the towers [Krehbiel et al., 2000, Thomas et al., 2004]. The LMA centroid was located southeast of the towers due to additional research objectives not related to UPLIGHTS. This location did, however, provide good 3-dimensional resolution of lightning generated source points for triggering and upward flashes from the towers. The

LMA system recorded and triangulated the peak amplitude very high frequency (VHF) emission in sequential 80  $\mu$ s time windows.

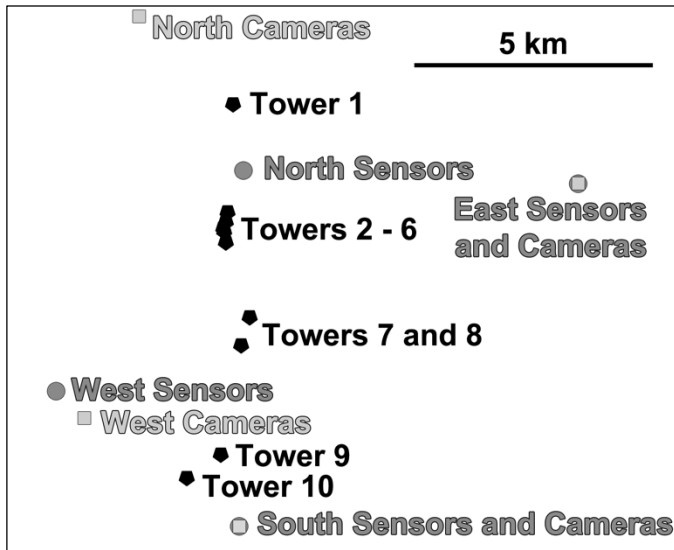


Figure 2. Layout of the 10 towers relative to the electric field sensing instrumentation and cameras.

National Lightning Detection Network (NLDN) stroke data [Cummins and Murphy, 2009] for a 200 km radius around the towers was obtained and analyzed for this study. Analysis provided timing and location of impulsive events detected by the NLDN during triggering and upward flashes.

The physics sign convention [Rakov and Uman, 2003, Section 1.4.2] will be used when referring to the electric field and its change. A positive electric field is an upward pointing field when the ground is positively charged and there is negative charge overhead. A positive field change would result if there were an increase in negative charge overhead.

### III. OBSERVATIONS

The UPLIGHTS formal observation timeframe fell within three summer thunderstorm seasons (Apr – Sep) from 2012 – 2014. A total of 38 upward flashes during 13 storms were observed from the 10 towers located in Rapid City. All 38 upward flashes were LTUL with the upward leaders being triggered by nearby preceding lightning activity. 37 upward flashes had upward propagating positive leaders develop from one or more towers, and we observed one upward flash in which an upward propagating negative leader developed from one tower. This was the first and only upward negative leader ever observed in Rapid City since observations began back in 2004.

18 of the 38 upward flashes (47%) had an upward positive leader develop from more than one tower during the flash. The maximum number of towers that initiated an UPL during a single upward flash was six and this occurred twice.

Four storms had only one upward flash occur and nine storms had more than one upward flash occur as it passed over the towers. The average number of upward flashes per storm

was 2.9 with a maximum of 8 upward flashes during a single storm.

### IV. VISUAL MODEL

Since UPLs are dominantly observed during LTUL in Rapid City, our visual model will focus on this type of upward flash, and we will address UNL triggering separately after the UPL cases. Our analysis suggests that two flash components are responsible for the initiation of UPLs from tall objects.

Firstly, negative leader development passing near or over the tall objects can create quasioleostatic stress at the tower tip due to the rapid positioning of negative charge near the towers that results in the initiation of an UPL. The addition of negative charge over the tower causes a positive field change as the electric field strengthens according to Coulomb’s Law. If this electric field strengthening occurs rapidly enough to overcome the increased induced positive corona space charge production near ground objects, which acts to reduce the sensed electric field at the tower tip, a self-propagating upward positive leader may form. This negative leader development can take place during an intracloud flash or prior to or after a positive cloud-to-ground (+CG) return stroke. Horizontally extensive flashes in MCSs, where negative leaders travel large distances through layered positive charge frequently found near cloud base, are the most effective in triggering UPLs [Mazur and Ruhnke, 2011; Warner, 2012; 2012a; 2012b; Saba et al., 2012, 2016; Schumann et al., 2014a, 2014b, 2014c]. Following a +CG return stroke, which effectively raises ground potential to the upper extent of the bidirectional leader network that formed prior to the return stroke, extensive negative leader growth can occur due to the potential difference between the upper extent of the return stroke channel (near ground potential) and the surrounding ambient cloud potential. The negative leader development can further extend previously formed leader channels and branches or create new branches which propagate in new directions as dictated by available charge regions (potential wells). This renewed development can travel large horizontal distances in the horizontally stratified positive charge regions frequently found in stratiform precipitation areas of MCSs [Lu et al., 2009]. As a result, the initiation time for an UPL may be well after the +CG return stroke if the renewed negative leader development has to travel significant distances to reach the tower area. The delay from a +CG return stroke to UPL initiation can exceed 100 ms [Warner et al., 2012a; Saba et al., 2016].

The second flash component that can trigger UPLs is the return stroke of a +CG flash. The return stroke, which effectively raises negative charge along the return stroke channel path, can again cause a large positive electric field change. If the return stroke channel path is near or over the towers, the speed of the return stroke and its associated quasioleostatic influence on the tower can again exceed the induced positive corona space charge production resulting in an UPL. Unlike the negative leader triggering flash component that can precede or follow a return stroke, the relatively short duration but intense field change associated with the return stroke results in a very short delay in initiating an UPL based on our observations, usually within 2 ms.

Analysis of the ambient electric field at the surface prior to upward flashes showed that it was preferentially positive. For

the 32 electric field records obtained near the towers, 27 (84%) showed a positive electric field prior to upward flash. Therefore, a fundamental question that must be addressed is how does the towers and ground obtain a positive induced charge when there is an overlying positive cloud charge region that serves as the potential well for horizontal negative leader propagation [Coleman et al., 2003, 2008]? It seems logical that upward positive leaders would form more easily if the tower had an induced positive charge at the time of the triggering flash so that the tower did not have to undergo a reversal from negative to positive induced charged from the influence of the triggering component prior to UPL initiation.

Figure 3 shows a simplified visual model that depicts the initial conditions prior to an upward flash. A stratiform precipitation area overlays the towers and contains a horizontally stratified positive charge region that is close to cloud base (Figure 3A). This positive charge region can advect downwind from the convective region of the storm and may contain areas of embedded weak convection [Stolzenburg et al., 1994; Carey et al., 2005]. Although originating from the upper tripole positive charge region found in the convective updraft portion of a normal polarity storm, the layered positive charge region found in the stratiform precipitation area typically has descended to a lower altitude near the melting layer [Shepherd et al., 1996].

Figure 3B shows that the presence of a layered positive charge region over the towers will likely result in induced negative charge in the ground and towers. Elevated objects such as towers and trees and buildings enhance the electric field locally and produce corona space charge that envelopes the region near the ground as shown in Figure 3C [Chauzy and Raizonville, 1982; Chauzy and Soula, 1989]. Due to the proximity of the negative corona space charge to the towers and the resulting reduction in tower-sensed electric field strength from the overlying in-cloud positive charge, the towers and nearby ground may experience a reduced induced charge and possibly even an induced charge reversal shown in Figure 3D. This would leave the towers with an induced positive charge as frequently seen prior to upward flashes. Furthermore, the possible formation of a negatively charged screening layer at cloud base due to the overlying positive cloud charge region [Zhou and Tinsley, 2007] could further support a positively induced ground and towers as shown in Figure 3E.

The possible contributions of negative corona space charge and negative screening layer to the favorable condition of induced positively charged towers needs to be further studied and characterized and should be a focus of future research. In the meantime, our visual model will contain the initial charge arrangement as presented.

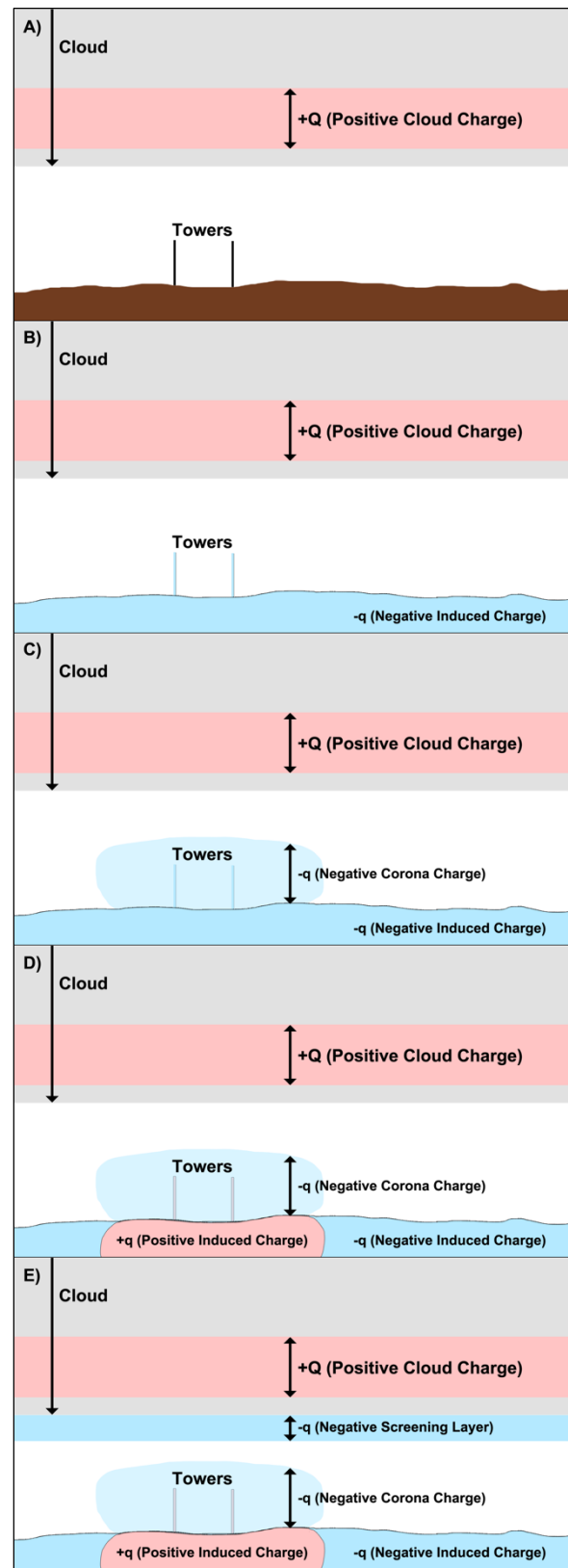


Figure 3. Initial conditions that prove favorable for the triggering of upward positive leaders.

*A. Intracloud Triggering Flash with Negative Leaders as Triggering Component (28 June 2014 – 23:47:15 UT)*

The first example will be an intracloud triggering flash in which the negative end of the bidirectional leader development passes over the towers. Based on analysis of LMA data, the initiation of this type of triggering flash typically occurs between the upper positive charge region and main negative charge region near the convective area of the storm. The negative leader development then follows the positive charge region as it slopes downward into the stratiform precipitation area and over the towers. For this scenario, the negative leaders simply pass over or near the towers and the increased positive electric field between the negative leaders and towers (which already enhances the electric field due to the towers' shape) exceeds a threshold for the initiation and development of an upward propagating positive leader (see Figure 4). The rapid quasioleostatic field change due to the approaching negative leaders and their associated negative charge likely exceeds the increasing screening effect due to the production of positive corona space charge production.

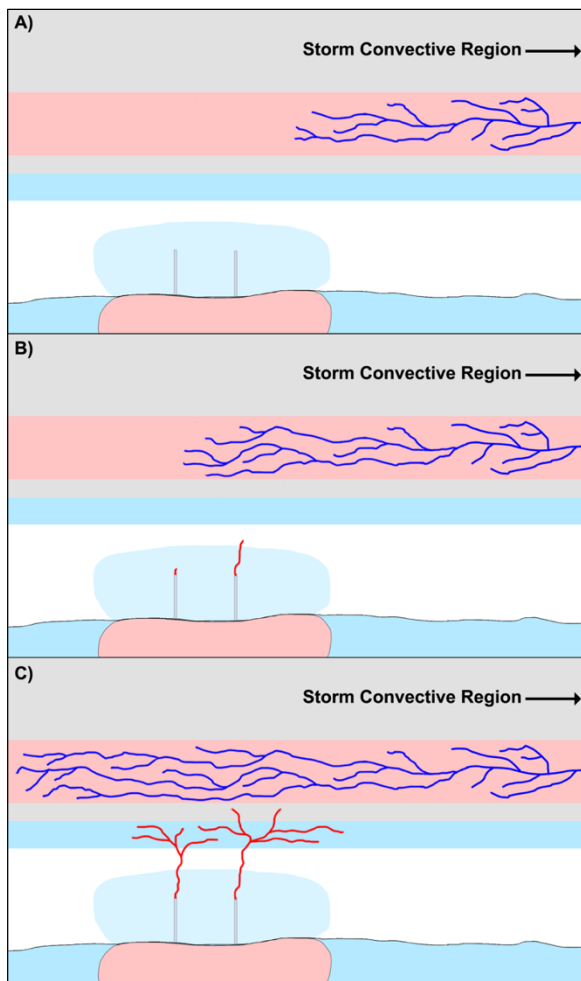


Figure 4. Visual model of an intracloud triggering flash with negative leaders as the triggering component. Positive charge in light red, negative charge in light blue, positive leaders in dark red and negative leaders in dark blue.

Figure 5 contains observed data from an intracloud triggering flash which initiated an UPL from a single tower. The flash initiated in the convective portion of a multicellular MCS with a small trailing stratiform precipitation area over the towers. The negative leader development initiated at 7 km above ground level (AGL) based on LMA data (right panels) and then traveled down to 4 km before passing over the towers. Visual in-cloud brightening, as recorded by a high-speed camera at the West Cameras site (upper left panels), traveled from right to left (south to north) over the towers prior to UPL initiation and correlated with the positive field change (lower left panels) and LMA-indicated VHF source points associated with negative leaders. Vertical red line in fast antenna and LMA data displays corresponds to time of high-speed video image.

*B. +CG Triggering Flash with Post Return Stroke Negative Leader Growth as Triggering Component (22 June 2014 – 02:24:08 UT)*

We next address how negative leader growth following a +CG return stroke can travel near a tall object and trigger an UPL. The visual model shown in Figure 6 begins with bidirectional leader development prior to the return stroke (Figure 6A). The return stroke, as shown in Figure 6B-D travels through the leader network formed prior to the return stroke. After the return stroke reaches the outer extent of the leader network (Figure 6D), new negative leader growth results in negative leaders passing near the towers and triggering UPLs as shown in Figure 6E-F.

Figure 7 contains an example of a +CG triggering flash in which post return stroke negative leader growth triggered an UPL from a single tower. The high-speed video recording from the East Camera location (upper left panels) had a view looking west toward the towers and triggering flash. The flash originated 66 km northwest of the towers at 10 km AGL with the negative leaders descending to 7 km after traveling 30 km to the southeast. The negative leaders remained at 7 km AGL while extending another 50 km southeast, remaining west of the towers by a minimum of 14 km.

This was followed by a +CG return stroke 21 km west of the towers and back along the path traveled by the negative leaders. The high-speed video recording of the +CG return stroke showed in-cloud brightening traversing the path previously taken by the negative leaders (see Figure 7A upper left panel and light blue south-pointed arrow in LMA display). This is followed by new negative leader growth from near the +CG return stroke location eastward toward the towers as shown in Figure 7B. As the negative leader growth passed near the towers, an UPL initiated as shown in high-speed video images in Figure 7B and 7C). The West electric field change sensor recorded the positive field change associated with the +CG return stroke (red line location in Figure 7A lower left panel), however it was the field change associated with the new negative leader growth that passed over the towers (red line location in Figure 7B lower left panel) that initiated the UPL. The delay time between the +CG return stroke and UPL initiation was 94 ms.

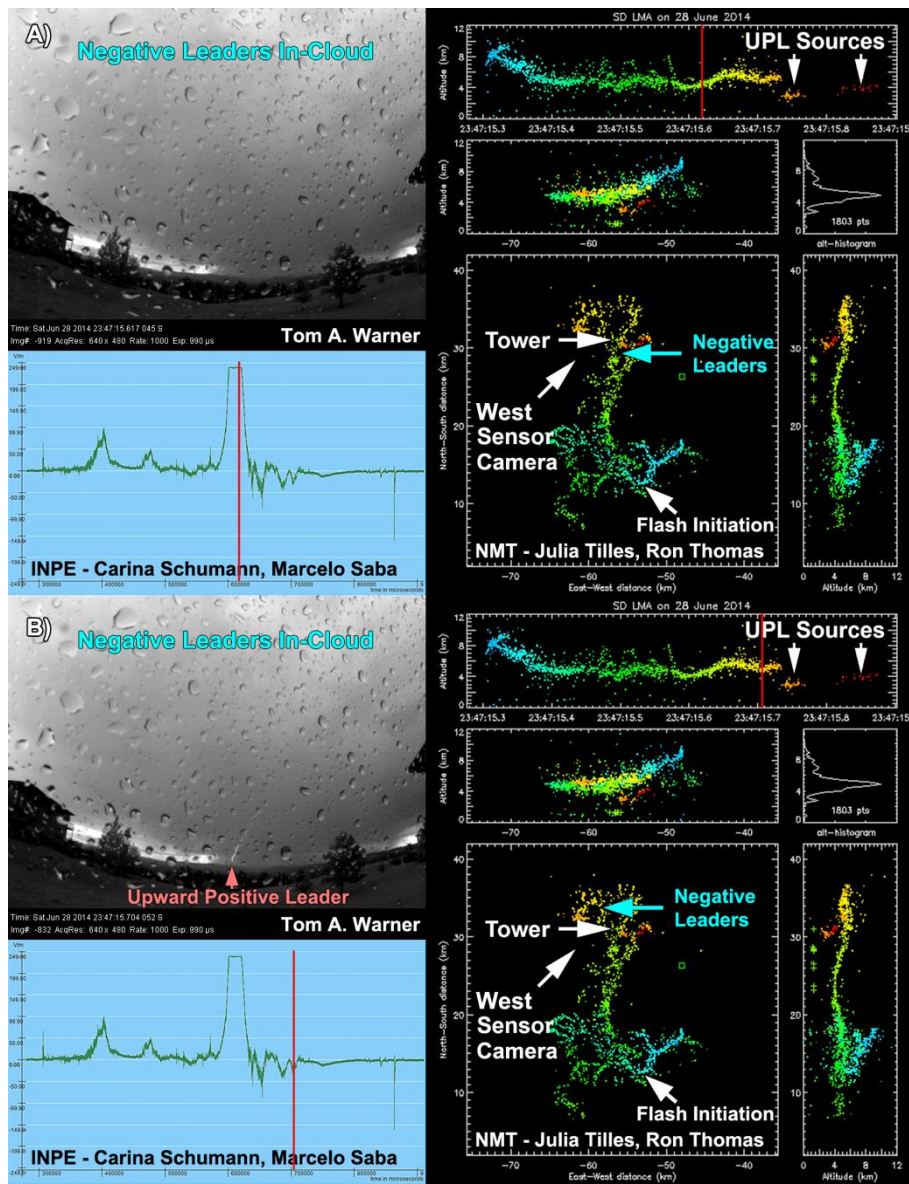


Figure 5. Composite figure showing images from a high-speed video recording (upper left panel), electric field change sensor recording (lower left panel) and LMA display (right panel). Red vertical lines show correlated time with high-speed video image.

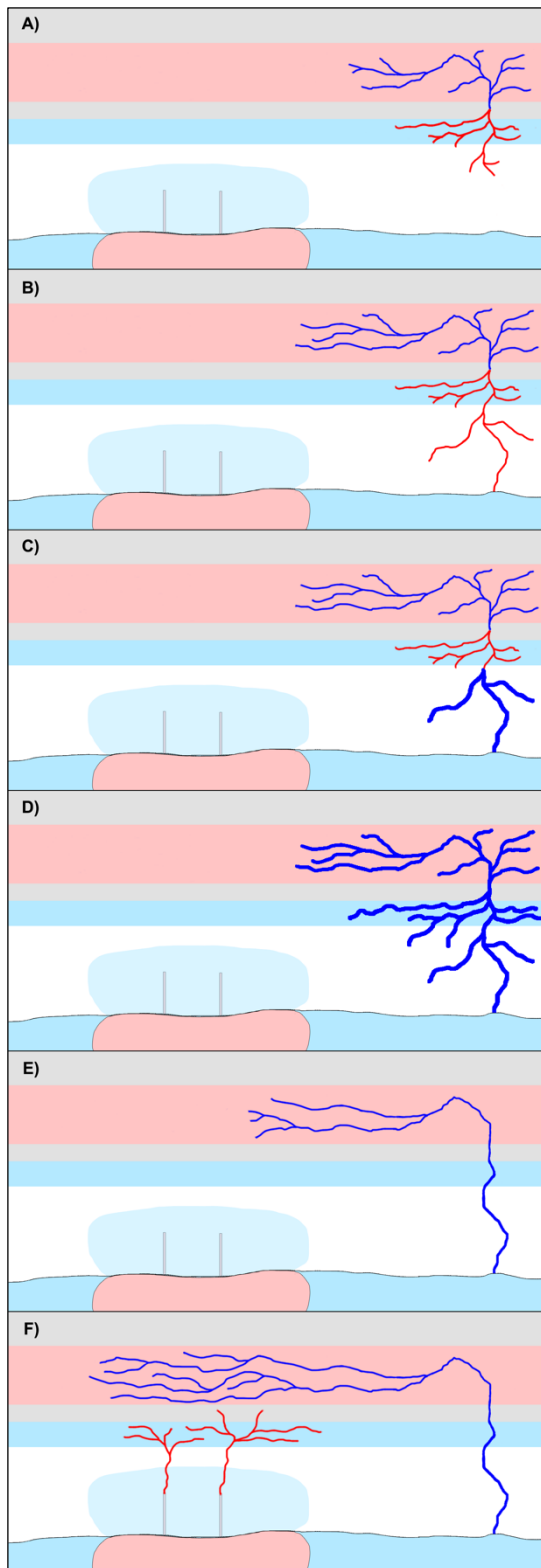


Figure 6. Visual model of +CG triggering flash with post return

stroke negative leader growth as the triggering component. Positive charge in light red, negative charge in light blue, positive leaders in dark red and negative leaders in dark blue. Return stroke is thickness enhanced dark blue.

*C. +CG Triggering Flash with Return Stroke as Triggering Component (1 June 2014 – 17:36:11 UT)*

If the negative portion of the bidirectional leader development that precedes a +CG return stroke forms near or over a tall object, the subsequent +CG return stroke can trigger an UPL. Our visual model for this process begins again with bidirectional leader development with the negative end passing over the towers as shown in Figure 8A and 8B. However, the electric field change associated with the approaching negative leaders does not trigger an UPL. The subsequent +CG return stroke traverses the leader network as shown in Figure 8C-F and the resulting electric field change from the rapid movement of negative charge near the towers results in the initiation of an UPL as shown in Figure 8E-F.

Figure 9 shows high-speed video recording images (upper left panel), fast electric field change record (lower left panel) and LMA display (right panel) of a +CG flash in which the return stroke triggered and UPL from two towers. The flash initiated 10 km east of the towers at an altitude of 4 km (Figure 9A LMA display) Negative leaders then traveled west over the towers which were visible as in-cloud brightening recorded by the high-speed video camera. Correspondingly, the West fast electric field change sensor recorded a positive field change as shown at the vertical red line location in Figure 9A. However, no UPLs initiated with the passage of the negative leaders. An NLDN-indicated -56.1 kA +CG return stroke 7.6 km east of the towers (light red plus in Figure 9B LMA display) resulted in a rapid positive field change as shown at the red line location of the field electric change recording in Figure 9B and there was a corresponding saturating brightness captured in the high-speed recording that traveled right to left (westward) as viewed from the South camera site. Two UPLs initiated within 2 ms of the return stroke one of which is visible in Figure 9C.

*D. -CG Triggering Flash with Return Stroke as Triggering Component for Upward Negative Leader (15 June 2015 – 02:00:01 UT)*

Over 11 years of upward flash observations, we have observed only one upward negative leader develop from the towers in Rapid City. The analysis of this flash indicated that a -CG return stroke triggered an UNL from a single tower. Figure 10 shows high-speed video images, electric field change and LMA display from this unique flash.

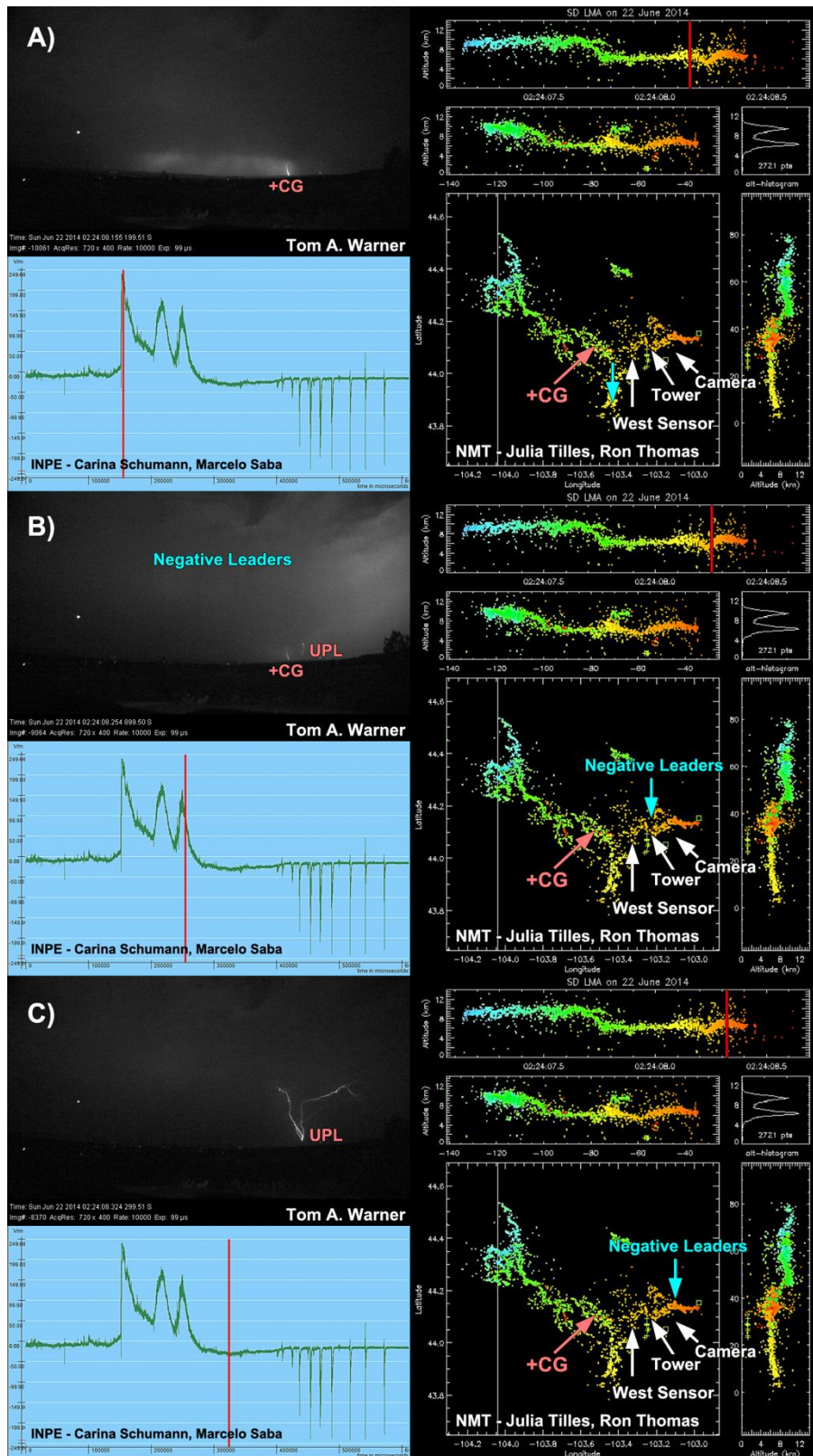


Figure 7 Composite figure showing images from a high-speed video recording (upper left panel), electric field change sensor recording (lower left panel) and LMA display (right panel). Red vertical lines show correlated time with high-speed video image.

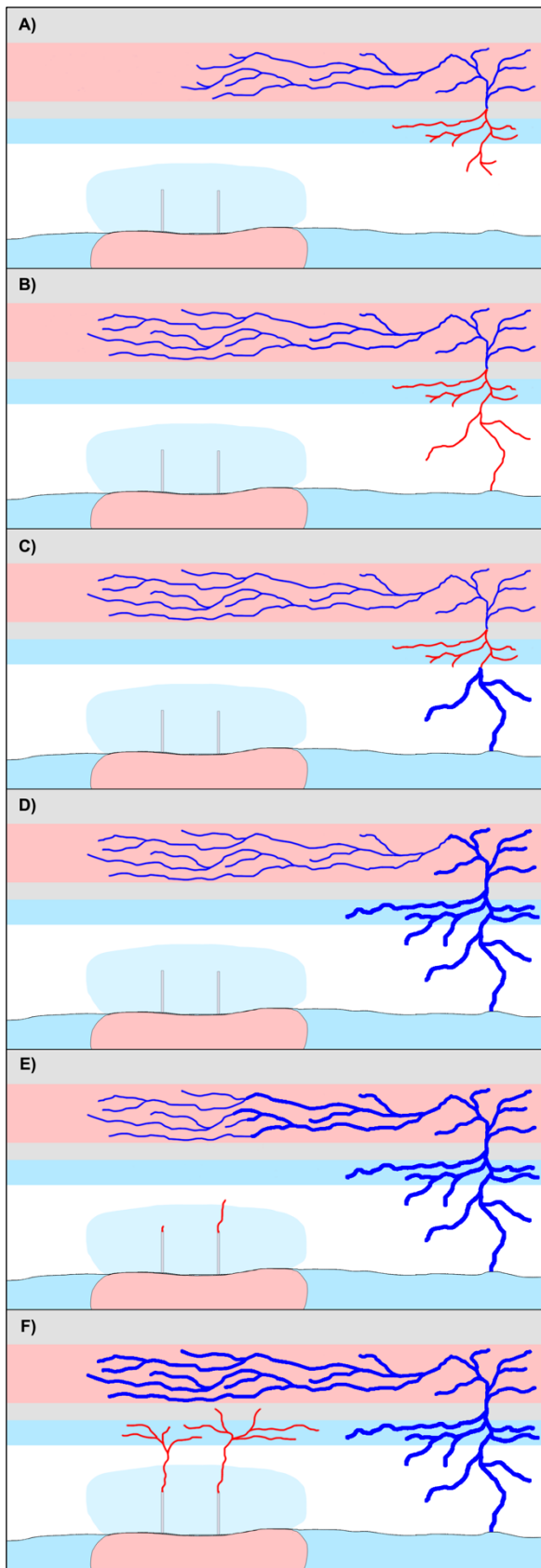


Figure 8. Visual model of +CG triggering flash with the return stroke as the triggering component. Positive charge in light red,

negative charge in light blue, positive leaders in dark red and negative leaders in dark blue. Return stroke is thickness enhanced dark blue.

Based on LMA data, the flash initiated at an altitude of 6 km, 15 km south-southwest of the tower. Negative leader development then propagated upward to 7 km while traveling west-southwestward for 10 km before descending to 4 km AGL while propagating westward for another 10 km. The negative leaders then remained at 4 km while traveling north-northeast for a total 50 km in a span of 350 ms. This was followed by visible negative leader activity below cloud base back near the flash origin. The LMA recorded corresponding VHF source points at 2 km AGL. A subsequent -CG return stroke 14 km southwest of the tower followed this activity.

An -14 kA estimated peak current IC event was recorded by the NLDN, but standard-speed video cameras captured the visible -CG return stroke channel as shown in Figure 11. The West electric field change sensor recorded a very large negative change associated with the return stroke as shown in Figure 10 (red line location in lower left panel) and saturating in-cloud brightness was correspondingly captured in the high-speed video recording along with the initiation of the UNL.

The upward propagating leader was clearly negative based on its visual behavior [Warner et al., 2016]. The leader tips stepped and exhibited chaotic directional change with branches remaining bright. The UNL propagated in the same direction as the post return stroke in-cloud brightness (north-northeast). The LMA recorded numerous VHF source points at 4 km immediately following the return stroke that spread primarily northward directly over the tower area. Based on the correlated negative field change response from the electric field sensors, these post return stroke leaders were positive polarity (see also [Edens et al., 2012]).

## I. DISCUSSION

For each upward flash, analysis of the correlated data resulted in the assignment of a triggering flash type and triggering component. Figure 12 shows the breakdown of triggering flash types for the 38 upward flashes. The +CG flash was the dominate triggering type at 76%.

Figure 13 shows the distribution of triggering flash components observed. Negative leaders triggered UPLs 29 times with 10 occurring during intracloud activity and 19 after a +CG return stroke. The +CG return stroke triggered one or more UPLs 12 times and a -CG return stroke triggered a single UNL. For three multiple upward leader flashes, multiple triggering components resulted in the initiation of UPLs from more than one tower during the same flash. This distribution suggests that although the +CG flash is the most favorable triggering flash type, negative leader activity passing near a tall object during intracloud development or after a +CG return stroke is 2.4 times more likely to initiate an UPL.

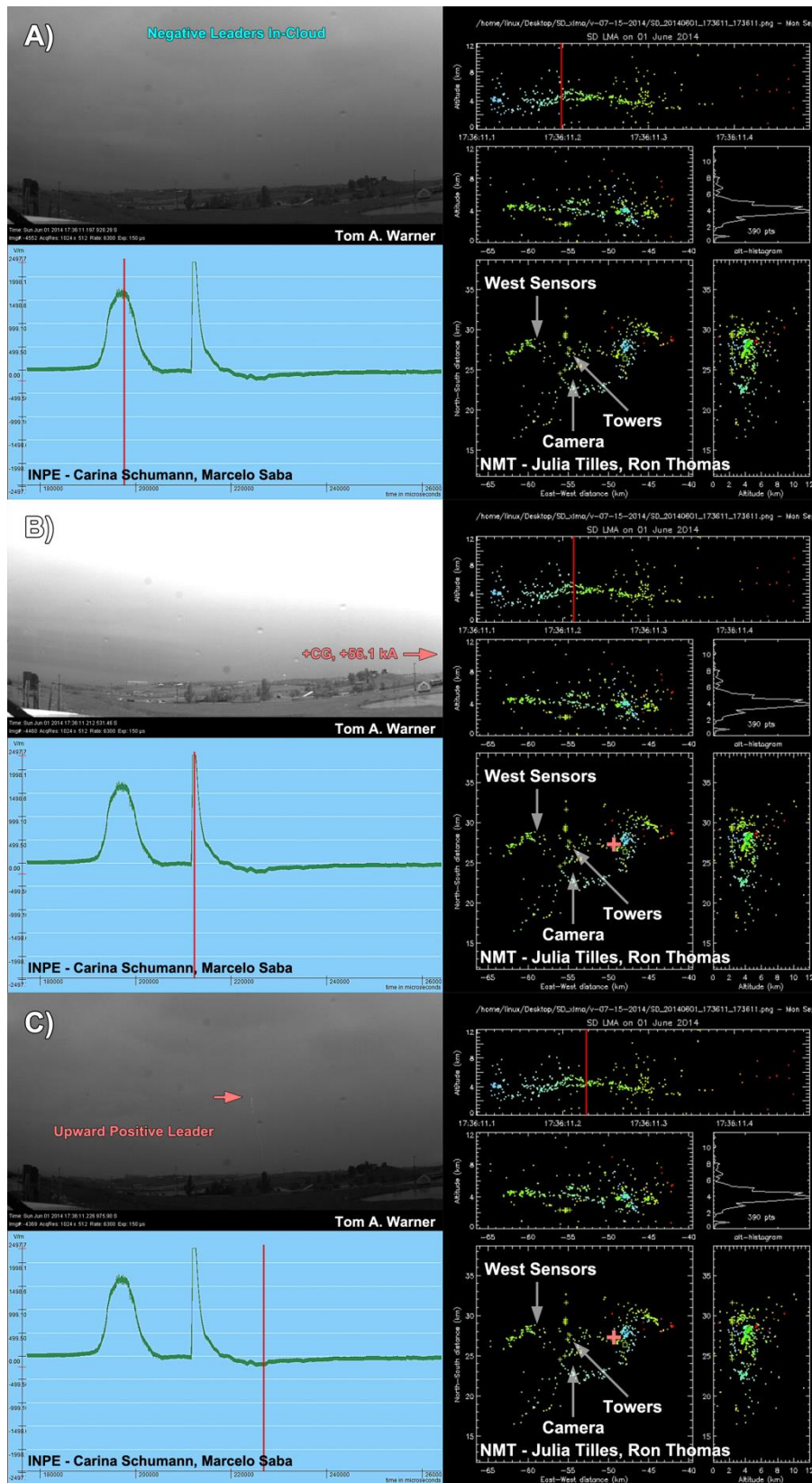


Figure 9. Composite figure showing images from a high-speed video recording (upper left panel), electric field change sensor recording (lower left panel) and LMA display (right panel). Red vertical lines show correlated time with high-speed video image.

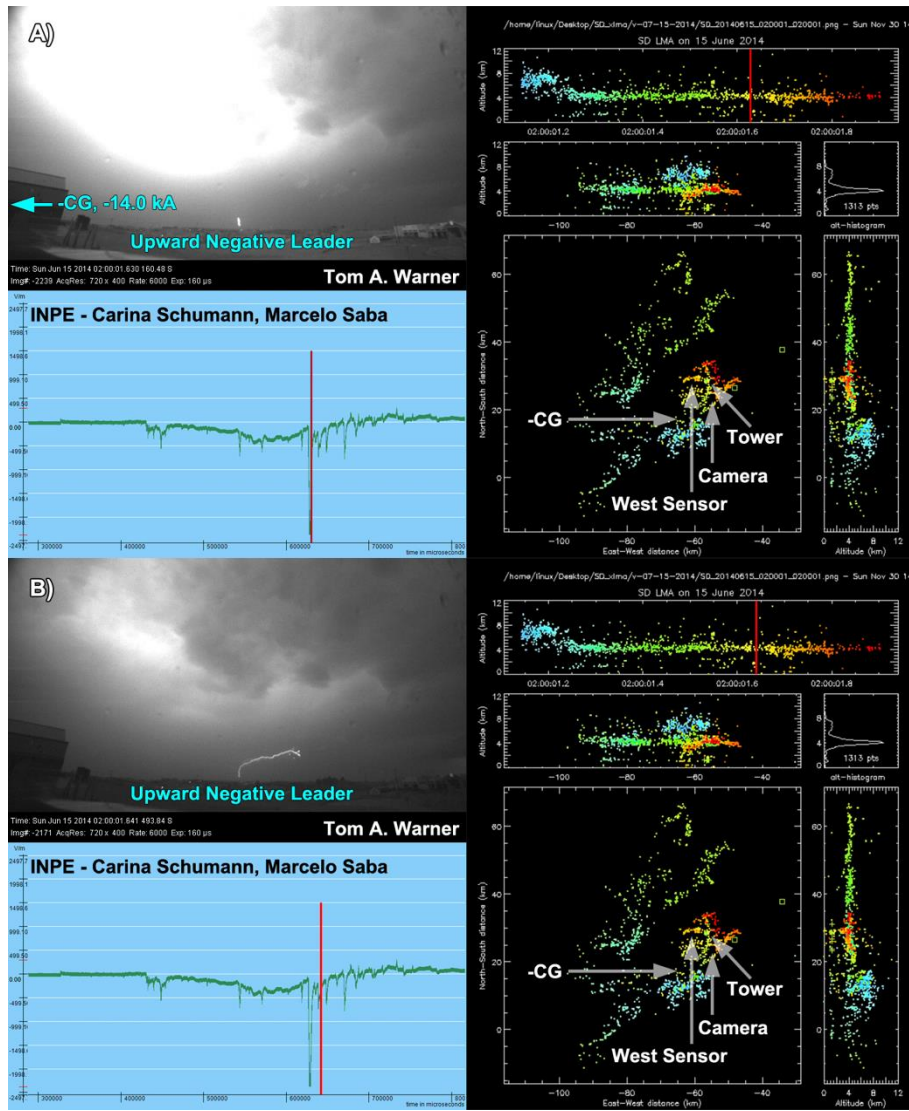


Figure 10. Composite figure showing images from a high-speed video recording (upper left panel), electric field change sensor recording (lower left panel) and LMA display (right panel). Red vertical lines in show correlated time with high-speed video image.



Figure 11. Standard-speed video image from East camera site showing triggering -CG return stroke channel and upward negative leader.

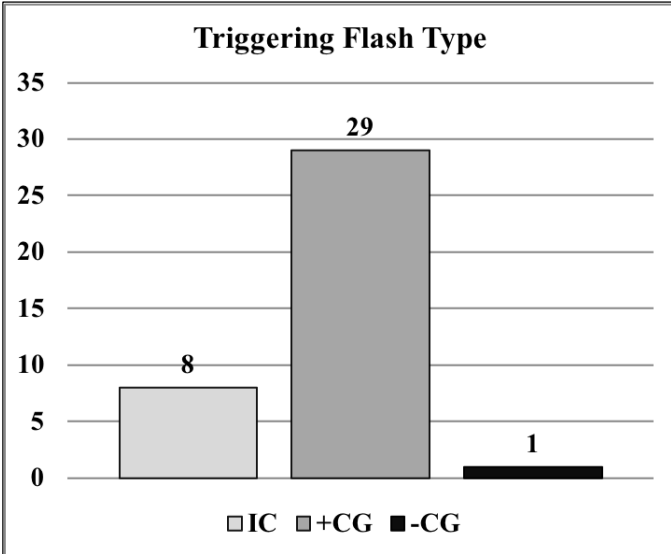


Figure 12. Histogram of triggering flash types.

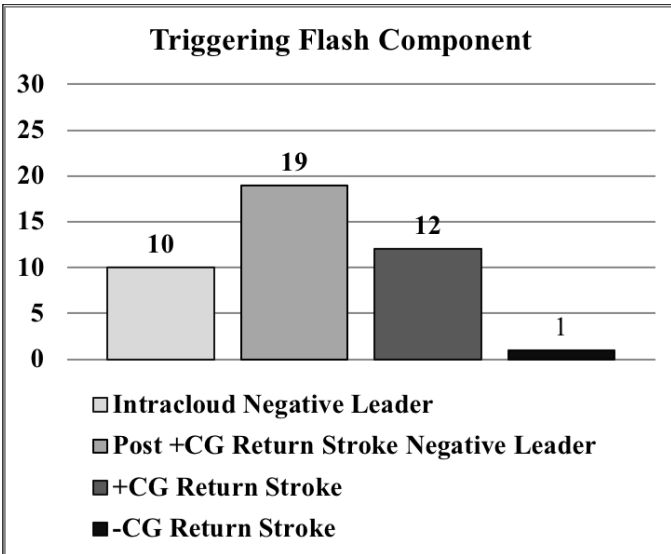


Figure 13. Histogram of triggering flash components observed for 38 upward flashes.

A notable observation regarding the triggered UNL was the magnitude of the recorded triggering negative field change relative to the typical positive field change magnitudes observed

during UPL triggering. Figure 14 shows the ambient electric field meter record for a typical upward flash in which an UPL develops. The black trace is the ambient electric field from the EFM closest to the towers located at the North Sensor site. It shows a positive ambient field prior to the triggering flash and then a positive electric field change associated with the triggering component. A electric field reversal due to the proximity of the developing UPL then follows. The blue trace from the mobile EFM located at the South Sensor site near the south towers shows a slightly positive ambient electric field and a triggering flash positive change. The red trace from the EFM at the West Sensor has a negative ambient field prior to the triggering flash (note that this site is 5 km west of the closest tower and typically upwind) and only records a triggering positive field change during the upward flash. Therefore, it appears that only the EFM close to the tower was significantly influenced by the UPL.

In contrast, the North Sensor site recorded an ambient negative electric field prior to the triggering upward flash in which a nearby UNL developed (see black trace in Figure 15). In fact the pre-flash ambient electric field recorded by all three EFMs are a near mirror opposite to that for the UPL case. All three EFMs recorded a very large negative electric field change associated with the triggering flash and no reversal due to the developing UNL. Given the extreme rarity of UNL flashes observed in Rapid City, this observation may suggest that only for cases of very large negative field change can an UNL initiate. This seems reasonable given the difference in breakdown electric field required for positive and negative leaders [Bazelyan and Raiser, 2000].

Analysis of UPLIGHTS data continues and additional findings will be reported in the future.

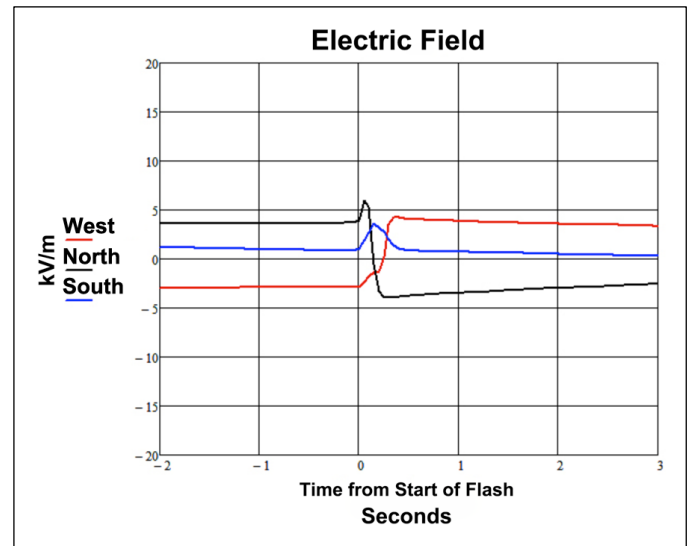


Figure 14. Ambient electric field meter recordings for an upward flash with an UPL. The red trace is from the West Sensor site EFM, the black trace is from the North Sensor site EFM, and the blue trace is from the South Sensor site EFM.

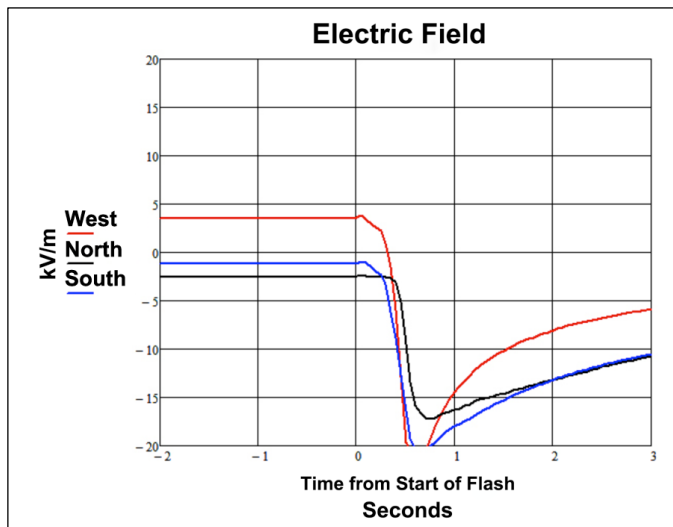


Figure 15. Ambient electric field meter recordings for an upward flash with an UNL. The red trace is from the West Sensor site EFM, the black trace is from the North Sensor site EFM, and the blue trace is from the South Sensor site EFM.

#### ACKNOWLEDGMENT

This research was made possible through National Science Foundation (NSF) grant AGS-1048103 and through FAPESP grants 2012/15375-7 and 2013/05784-0. Additionally, NSF grant ATM – 0813672 provided funding for concurrent high-speed optical spectra observations during UPLIGHTS. We would like to thank Dr. Walt Lyons for his help with forecasting and insight and expertise into the development of horizontally extensive flashes. We would also like to acknowledge Chip Redmond, John Hamilton, Jeferson Alves and Dan McKemy for their participation in the collection of data during UPLIGHTS. A special thank you to Mike Bickett for his many contributions in the fabrication, installation and maintenance of equipment and housings used during UPLIGHTS and to Seth White, Eddie and Marty Rypkema, Pete Lein, Kim Kjerstad, Rick MacDonald, Bill Kopp, Travis Madsen, Quiten Feickert, Dan Holsworth and Jim Bickett for the use of their land for sensors and observations. The data collected during UPLIGHTS is maintained by and available upon request from Tom A. Warner, tom.warner@ztresearch.com. A duplicate copy of this data is maintained by Marcelo Saba, Ph.D., marcelo.saba@inpe.br and Carina Schumann, Ph.D., carina.schumann@gmail.com.

#### REFERENCES

Bazelyn, E. M, and Y. P. Raizer (2000), *Lightning Physics and Lightning Protection*, Institute of Physics Publishing, Bristol

Carey, L. D., M. J. Murphy, T. L. McCormick, and N. W. S. Demetriades (2005), Lightning location relative to storm structure in a leading-line, trailing-stratiform mesoscale convective system, *J. Geophys. Res.*, 110, D03105, doi:10.1029/2003JD004371.

Chauzy, S., and P. Raizonville (1982), Space charge layers created by coronae at ground level below thunderclouds: Measurements and modeling, *J. Geophys. Res.*, 87(C4), 3143–3148.

Chauzy, S., and S. Soula (1989), Ground coronae and lightning, *J. Geophys. Res.*, 94(D11), 13,115–13,119.

Coleman, L. M., T. C. Marshall, M. Stolzenburg, T. Hamlin, P. R. Krehbiel, W. Rison, and R. J. Thomas (2003), Effects of charge and electrostatic potential on lightning propagation, *J. Geophys. Res.*, 108(D9), 4298, doi:10.1029/2002JD002718.

Coleman, L. M., M. Stolzenburg, T. C. Marshall, and M. Stanley (2008), Horizontal lightning propagation, preliminary breakdown, and electric potential in New Mexico thunderstorms, *J. Geophys. Res.*, 113, D09208, doi:10.1029/2007JD009459.

Cummins, K. L., and M. J. Murphy (2009), An Overview of Lightning Locating Systems: History, Techniques, and Data Uses, With an In-Depth Look at the U.S. NLDN, *IEEE Trans. Electromag. Compat.*, 51(3), 499-518.

Edens, H. E., K. B. Eack, E. M. Eastvedt, J. J. Trueblood, W. P. Winn, P. R. Krehbiel, G. D. Aulich, S. J. Hunyady, W. C. Murray, W. Rison, S. A. Behnke, and R. J. Thomas (2012), VHF lightning mapping observations of a triggered lightning flash, *Geophys. Res. Lett.*, 39, L19807, doi:10.1029/2012GL053666.

Jiang, R., X. Qie, Z. Wu, D. Wang, M. Liu, G. Lu and D. Liu (2014), Characteristics of upward lightning from a 325-m-tall meteorology tower, *J. Atmos. Res.*, 149, pp. 111-119, doi:10.1016/j.atmosres.2014.06.007

Krehbiel, P. R., R. J. Thomas, W. Rison, T. Hamlin, J. Harlin and M. Davis (2000), GPS-based mapping system reveals lightning inside storms, *Eos, Trans. Am. Geophys. Union*, 81, 21.

Lu, G., S. A. Cummer, J. Li, F. Han, R. J. Blakeslee, and H. J. Christian (2009), Charge transfer and in-cloud structure of large-charge-moment positive lightning strokes in a mesoscale convective system, *Geophys. Res. Lett.*, 36, L15805, doi:10.1029/2009GL038880.

Lyons, W. A., S. A. Cummer, S. A. Rutledge, T. J. Lang, T. Meyer, T. A. Warner, and T.A. Samaras (2011), TLEs and their parent lightning discharges, paper presented at 14th Intl. Conf. on Atmospheric Electricity, August 7-12, Rio De Janeiro, Brazil, 4 pp.

Lyons, W. A., T. A. Warner, S. A. Cummer, S. A. Rutledge, T. J. Lang, T. C. Meyer, G. Lu, T. E. Nelson, and T. Samaras (2012) Different strokes: Researching the unusual lightning discharges associated with sprites and jets and atypical meteorological regimes, paper presented at the 22nd Intl. Lightning Detection Conf., Broomfield, CO, Vaisala, Inc., www.vaisala.com/en/events/ildcilmc/ Pages/ILDC-2012-archive.aspx

Lyons, W. A., T.E. Nelson, T.A. Warner, T.J. Lang, K. Cummins, M. Quick, W. Rison, P. Krehbiel, S.A. Cummer, J. Myers, T. Samaras, P. Samaras, C. Young (2014), Meteorological Aspects of Two Modes of Lightning Triggered Upward Lightning (LTUL) Events in Sprite-Producing MCSs , paper presented at the 23rd International Lightning Detection Conference, Mar 18 - 19, Tucson, Arizona.

Miki, M., T. Miki, A. Wada, A. Asakawa, Y. Asuka and N. Honjo (2010), Observation of lightning flashes to wind turbines, Proceedings of the 30th International Conference on Lightning Protection, Sep 13-17, Cagliari, Italy.

Mazur, V., and L. H. Ruhnke (2011), Physical processes during development of upward leaders from tall structures, *J. Electrostatics*, 69, 97-110.

- Rakov, V. A., and M. A. Uman (2003), *Lightning: Physics and Effects*, Cambridge Univ. Press, New York.
- Rison, W., R. Thomas, P. Krehbiel, D. Rodeheffer, K. Cummins, M. Quick, J. Myers, T. Warner, M. Saba, C. Schumann, W. Lyons, T. Samaras, P. Samaras, C. Young, S. Cummer, G. Lu (2014), LMA and Slow Antenna Observations of Naturally Induced Upward Positive Leaders from Wind Turbines, paper presented at the 23rd International Lightning Detection Conference, Mar 18 - 19, Tucson, Arizona.
- Saba, M. M. F., J. Alves, C. Schumann, D. R. Campos and T. A. Warner (2012), Upward Lighting in Brazil. Paper presented at the 22nd International Lightning Detection Conference, Apr 2 – 5, Boulder, Colorado, USA
- Saba, M. M. F., C. Schumann, T. A. Warner, M. A. S. Ferro, A. R. de Paiva, J. Helsdon Jr, and R. E. Orville (2016), Upward lightning flashes characteristics from high-speed videos, *J. Geophys. Res. Atmos.*, 121, doi:10.1002/2016JD025137.
- Schumann, C., M. M. F. Saba, A. R. de Paiva, R. Jaques M. A. da Silva Ferro, T. A. Warner, (2014a), High-Speed Observation of Upward Lightning Flashes in Brazil, paper presented at the 23rd International Lightning Detection Conference, Mar 18 - 19, Tucson, Arizona.
- Schumann, C., M. M. F. Saba, M. A. da Silva Ferro, T. A. Warner, A. R. de Paiva, and R. Jaques (2014b), Mechanism of Triggering Upward Lightning from Towers in São Paulo, Brazil, paper presented at the International Conference on Grounding and Earthing and 6th International Conference on Lightning Physics and Effects, Manaus, Brazil, May 2014.
- Schumann, C., M. M. F. Saba, A. R. de Paiva, R. Jaques, W. Schulz, G. Diendorfer, M. A. da Silva Ferro, and T. A. Warner (2015), Analysis of terrain and atmospheric conditions for upward flashes in Sao Paulo-Brazil, paper presented at XIII International Symposium on Lightning Protection (SIPDA), Balneario Camboriu, Brazil, 28 Sep – 2 Oct.
- Shepherd, T.R., W.D. Rust, and T.C. Marshall (1996) Electric Fields and Charges near 0°C in Stratiform Clouds. *Mon. Wea. Rev.*, 124, 919–938, [https://doi.org/10.1175/1520-0493\(1996\)124<0919:EFACNI>2.0.CO;2](https://doi.org/10.1175/1520-0493(1996)124<0919:EFACNI>2.0.CO;2)
- Smorgonskiy, A., A. Tajalli, F. Rachidi, M. Rubinstein, G. Diendorfer, H. Pichler (2015), An analysis of the initiation of upward flashes from tall towers with particular reference to Gaisberg and Säntis Towers, *J. Atmos and Solar-Terr. Phys.*, DOI: 10.1016/j.jastp.2015.06.016
- Stolzenburg, M., T. C. Marshall, W. D. Rust, and B. F. Smull (1994), Horizontal distribution of electrical and meteorological conditions across the stratiform region of a mesoscale convective system. *Mon. Weather Rev.*, 122, 1777–1797, doi:10.1175/1520-0493(1994)122<1777:HDOEAM>2.0.CO;2.
- Thomas, R. J., P. R. Krehbiel, W. Rison, S. J. Hunyady, W. P. Winn, T. Hamlin and J. Harlin (2004) Accuracy of the Lightning Mapping Array, *J. Geophys. Res.*, doi:10.1029/2004JD004549.
- Wang, D., N. Takagi, T. Watanabe, H. Sakurano, and M. Hashimoto (2008), Observed characteristics of upward leaders that are initiated from a windmill and its lightning protection tower, *Geophys. Res. Lett.*, 35, L02803, doi:10.1029/2007GL032136.
- Wang D., and N. Takagi (2012), Three Unusual Upward Positive Lightning Triggered by Other Nearby Lightning Discharge Activity, paper presented at the 22nd International Lightning Detection Conference, 2 – 3 April, Broomfield, Colorado, USA
- Warner, T. A. (2012), Observations of simultaneous upward lightning leaders from multiple tall structures, *Atmos. Res.*, 117, 45–54, doi:10.1016/j.atmosres.2011.07.004.
- Warner, T. A., K. L. Cummins, and R. E. Orville (2012a), Upward lightning observations from towers in Rapid City, South Dakota and comparison with National Lightning Detection Network data, 2004–2010, *J. Geophys. Res.*, 117, D19109, doi:10.1029/2012JD018346.
- Warner, T. A., M. M. F. Saba, S. Rudge, M. Bunkers, W. A. Lyons, and R. E. Orville, (2012b), Lightning-triggered upward lightning from towers in Rapid City, South Dakota, paper presented at the 2012 International Lightning Detection Conference, Apr 2 – 3, Boulder, Colorado.
- Warner, T. A., M. M. F. Saba, and R. E. Orville (2012c), Characteristics of Upward Leaders from Tall Towers, paper presented at the 22nd International Lightning Detection Conference, Apr 2 – 3, Boulder, Colorado.
- Warner, T. A., J. H. Helsdon Jr., M. J. Bunkers, M. M. F. Saba, and R. E. Orville (2013), UPLIGHTS – Upward Lightning Triggering Study, *Bull. Amer. Meteor. Soc.*, 94(5), 631-635.
- Warner, T. A., M. M. F. Saba, C. Schumann, J. H. Helsdon Jr., and R. E. Orville (2016), Observations of bidirectional lightning leader initiation and development near positive leader channels, *J. Geophys. Res. Atmos.*, 121, 9251–9260, doi:10.1002/2016JD025365.
- Zhou, L., and B. A. Tinsley (2007), Production of space charge at the boundaries of layer clouds, *J. Geophys. Res.*, 112, D11203, doi:10.1029/2006JD007998.
- Zhou, H., G. Diendorfer, R. Thottappillil, H. Pichler, and M. Mair (2012), Measured current and close electric field changes associated with the initiation of upward lightning from a tall tower, *J. Geophys. Res.*, 117, D08102, doi:10.1029/2011JD017269.
- Yuan, S., R. Jiang, X. Qie, D. Wang, Z. Sun and M. Liu, (2017), Characteristics of upward lightning on the Beijing 325 m meteorology tower and corresponding thunderstorm conditions, in press, doi: 10.1002/2017JD027198